A CHALLENGING TURBULENT MAGNETIC SUN

Allan Sacha Brun

DSM/DAPNIA/SAp & UMR AIM 7158, CEA-Saclay, 91191 Gif-sur-Yvette, Cedex

ABSTRACT

We discuss recent advances made in modelling in three dimensions the internal magnetohydrodynamical processes present in the Sun with the anelastic spherical harmonic (ASH) code. We focus our study on how dynamical processes in stable (radiative) or unstable (convective) zones, nonlinearly interact with magnetic field under the influence of rotation to establish the solar differential rotation, meridional circulation, confine the tachocline and amplify and organize magnetic fields. The intense magnetism of the Sun is most likely linked to dynamo action in the turbulent convective envelope. We show that the associated Maxwell and Reynolds stresses present in such an intense magnetized turbulent layer, play an important role in setting the solar differential rotation helped by baroclinic forcing at the base of the convection zone. Such convective layers generate strong non-axisymmetric and intermittent fields and weak mean (axisymmetric) fields, but do not possess a regular cyclic magnetism. A possible resolution of these difficulties seems to rely in the presence of the solar tachocline at the base of the convection zone, which can potentially amplify and organize the solar magnetic fields and shape the large scale mean flows.

Key words: Sun: Convection, Turbulence, Rotation, Magnetism, Dynamo; MHD.

1. THE OBSERVATIONAL CONSTRAINTS

The Sun's surface and hot atmosphere exhibits a wide range of magnetohydrodynamical processes, which for the most part are related and dynamically linked to the complex interactions between its turbulent surface convection, rotation and magnetic fields. The magnetic fields, like the underlying turbulence, can be both orderly on some scales and chaotic on others. Most striking is that the Sun exhibits 22-year cycles of global magnetic activity, involving sunspot eruptions with very well defined rules for field parity and emergence latitudes as the cycle evolves. Coexisting with these large-scale ordered magnetic structures are small-scale but intense magnetic fluctuations that emerge over much of the solar surface, with little regard for the solar cycle. This diverse range of activity is summarized in the following list (see also Judge 2003, Charbonneau 2005):

- An activity cycle of 22 yr (Schwabe's cycle), 11 yr for the sunspots, an amplitude modulation of 90-100 yr (Gleissberg), and the occurence ($\sim$ 200 yr) of grand minima of activity (Maunder, Sporer),
- Butterfly diagram (Sporer's law) of the toroidal field within a latitudinal band of +/- 35°, with the existence of so-called active longitudes, separated by 180°, as the site of emergence of new active regions
- Tilt of 4 to 10° of bipolar regions (Joy's law), opposite polarity between northern and southern hemisphere for leading spot (Hale's law)
- Poloidal field migrating from mid latitudes towards the poles 90 deg phase shift between polar surface field and deep toroidal field, such that the polar field reverses ($- \rightarrow +$) when Btor is at maximum strength (+)
- Btor $\sim 3\ 10^3$ G in sunspots, 10^4-10^5 G indirectly estimated via seismic inversion in the tachocline, Bpol $\sim$ 10 G at poles (surface amplitude)
- Large and small scale dynamos, with for the latter, the existence of brigth points and intergranular magnetic flux
- Solar flares, CME's, prominences, witht their intensity/occurence being related to the activity cycle
- A hot extended corona ($\sim 1 - 2\ 10^6$ K) changing into a slow or fast (above coronal holes) solar wind, further delimiting the heliosphere

The origin of the observed solar magnetic fields must rest with dynamo processes occurring deep within the star in the spherical shell of intensely turbulent convection that occupies the outer 29% in radius below the solar surface. Within this convection zone, complex interactions

between compressible turbulence and rotation of the star serve to redistribute angular momentum so that a strong differential rotation is achieved. Further, since the fluid is electrically conducting, currents will flow and magnetic fields must be built. Yet there are many fundamental puzzles about the dynamo action that yields the observed fields. The observed large diversity of magnetic phenomena must thus be linked to two conceptually different dynamos: a large-sclae/cyclic dynamo and a turbulent small scale one (e.g., Weiss 1994; Cattaneo & Hughes 2001; Ossendrijver 2003).

2. A LIKELY THEORETICAL MODEL FOR THE GLOBAL DYNAMO

The operation of the solar global dynamo appears to involve many dynamical elements, including the generation of fields by the intense turbulence of the deep convection zone, the transport of these fields into the tachocline region near the base of the convection zone, the storage and amplification of toroidal fields in the tachocline by differential rotation, and the destablization and emergence of such fields due to magnetic buoyancy. Self-consistent magnetohydrodynamic (MHD) simulations which realistically incorporate all of these processes are not yet computationally feasible, though some elements can now be studied with reasonable fidelity.

The pairing of opposite polarity sunspots in the east-west direction within active regions is most readily interpreted as the surface emergence of large-scale toroidal field structures. These structures are created somewhere below the photosphere and rise upwards, bending to pierce the photosphere in the form of curved tubes. The current paradigm for large-scale dynamo action (e.g., Parker 1993) involves two major components. First, strong toroidal field structures must be generated. This is believed to occur due to the stretching that any differential rotation in latitude or radius will impose on any weak existing poloidal field. This first process is often referred to as the ω-effect after its parameterization within the framework of mean-field electrodynamics (Moffatt 1978). Helioseismology has shown that gradients in angular velocity are particularly strong in the tachocline, pointing to this interface region between the convection zone and the deeper radiative interior as the likely site for the generation of strong toroidal fields. Second, an inverse process is required to complete the cycle, regenerating the poloidal field from the toroidal field. Different theories exist for the operation of this process (known as the α-effect). Some have the poloidal field regenerated at the surface through the breakup and reconnection of the large-scale field that emerges as active regions, where this field has gained a poloidal component due to Coriolis forces during its rise, with meridional flows having a key role in transporting such flux both poleward and down toward the tachocline (e.g. Dikpati & Charbonneau 1999). Others believe that the poloidal field is regenerated by the cumulative action of many small-scale cyclonic turbulent motions on the field throughout the convection zone, rather than just close to the surface (e.g., Parker 1993). In either scenario, there is separation in the sites of generation of toroidal field (in the strong shear of the tachocline) and regeneration of poloidal field (either near the surface or in the bulk of the convection zone), yielding what is now broadly called an *interface dynamo* (Parker 1993).

The interface dynamo paradigm is thus based on the following underlying processes or building blocks: (a) The α-effect: the generation of the background weak poloidal field, either by cyclonic turbulence within the convection zone or by breakup of active regions. (b) The β-effect or turbulent transport: the transport of the weak poloidal field from its generating region to the region of strong shear, the tachocline (either by meridional flows or turbulent convective plumes (Tobias et al. 2001)). (c) The ω-effect: the organization and amplification of the magnetic field by differential rotation, particularly by large-scale rotational shear in the tachocline, into strong, isolated magnetic structures that are toroidal in character. (d) Magnetic buoyancy: the rise and transport of the large-scale toroidal field by magnetic buoyancy into and through the convection zone to be either shredded and recycled or to emerge as active regions.

The interface dynamo scenario has not always been the favoured explanation of the solar magnetic cycle and activity. A distributed dynamo operating only in the convection has also been considered (Stix 1976, Gilman 1983) but helioseismic inversions of a solar conical angular velocity in the early 80's (see Thompson et al. 2003) forced the communauty to develop the interface dynamo model. More recently though, Brandenburg (2005) has proposed a revised version of the distributed dynamo scenario. However, we personally think in regards of our numerical results that the interface dynamo is a more likely scenario given the fact that for example it explains quite naturally the generation and emergence (following the well established butterfly diagram) of sunspots, while in purely convective models the mean toroidal fields can never seem to be amplified and stored long enough to form an 11 yr cycle. Nevertheless it is alwyas very useful and instructive to compared both solar dynamo models (distributed vs interface) in the light of new theoretical, numerical or observational results to verify which one remains the most likely to explain the solar (large scale) magnetism.

3. NUMERICAL SIMULATIONS OF THE SOLAR INTERNAL MAGNETOHYDRODYNAMICS

We use the ASH code (anelastic spherical harmonic; see Clune et al. 1999, Miesch et al. 2000, Brun, Miesch & Toomre 2004 (hereafter BMT04)), to solve the full set of 3–D MHD anelastic equations of motion (Glatzmaier 1987) in a rotating, convective or radiative spherical shell with high resolution on massively-parallel computing architectures. The anelastic approximation captures the effects of density stratification without having to resolve sound waves which would severely limit the time step. In the MHD context, the anelastic approximation filters out

fast magneto-acoustic waves but retains the Alfvén and slow magneto-acoustic modes.

Due to limitations in computing resources, no simulation achievable now or in the near future can hope to directly capture all scales present in the Sun from global to molecular dissipation scales. Our models should be regarded as large-eddy simulations (LES) with parameterizations to account for subgrid-scale (SGS) motions, with effective eddy diffusivities ν, κ, and η representing momentum, heat, and magnetic field transport by motions which are not resolved by the simulation. These quantities are allowed to vary with radius but are independent of latitude, longitude, and time for a given simulation. In order to ensure that the mass flux and the magnetic field remain divergenceless to machine precision throughout the simulation, we use a toroidal–poloidal decomposition (see BMT04).

3.1. Magnetized Convection

Our numerical model is a highly simplified description of the solar convection zone: solar values are taken for the heat flux, rotation rate, mass and radius, and a perfect gas is assumed. The computational domain extends from 0.72 to 0.97 $R_\odot$ (or $L = 1.72 \times 10^{10}$ cm), thereby concentrating on the bulk of the unstable zone and here not dealing with neither penetration into the radiative interior nor convective motions in the near surface shear layer. We have computed purely hydrodynamical (such as cases H, AB or AB3) or MHD (such as M3) models of the solar convection zone in which we have varied some of the control parameters (such as the Rayleigh, Reynolds and Prandtl numbers) or boundary conditions (BCs) (see Brun & Toomre 2002, BMT04, Miesch, Brun & Toomre 2005 for futher details).

Figure 1 shows the kinetic and magnetic energy time traces over 4000 days of simulated time of case *M3* We see that the magnetic energy (ME) grows by many order of magnitude through dynamo action. After 1200 days, the ME saturates, due to the nonlinear feed back of the Lorentz forces, to a value of about 7% of the KE and retains that level for more than 3 ohmic decay times. Upon saturation, the kinetic energy (KE) in the model has been reduced by about 40% compared to its initial value, say KE_0, given by case H. This change is mostly due to a reduction of the energy contained in the differential rotation (DRKE) which drops by over 50%. By contrast, the energy contained in the convective motions (CKE) only decreases by about 27%, which implies an increased contribution of the non-axisymmetric motions to the total kinetic energy balance. For case *M3*, the decrease in KE first becomes apparent after about 600 days of evolution, when the ME reaches roughly 0.5% of KE_0, attaining a value larger than that contained in the meridional circulation kinetic energy (MCE).

The total kinetic and magnetic energies are small compared to the total potential, internal and rotational energies contained in the shell. The magnetic energy must

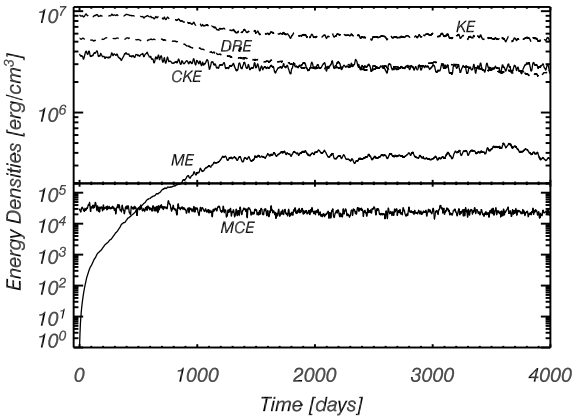

Figure 1. Kinetic (KE) and magnetic energy (ME) time traces for case M3. Also shown are the kinetic energies contained in meridional flows (MCE), differential rotation (DRE) and non axisymmetric convective motions (CKE). Note the significant decrease of DRE as ME grows and becomes larger than MCE.

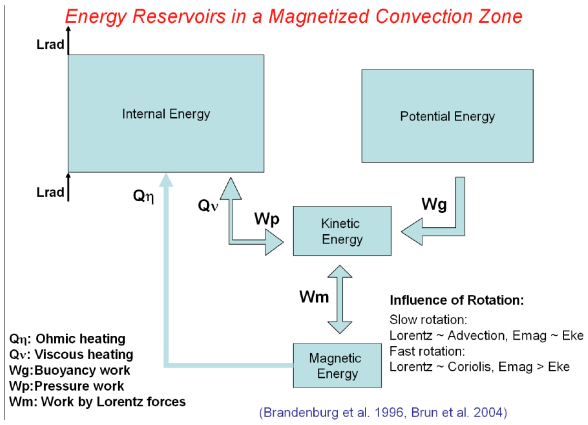

Figure 2. Energy reservoirs

arise from the conversion of kinetic energy but this does not necessarily lead to a decrease in the total kinetic energy because the motions may draw upon the other reservoirs (see Figure 2). Yet, in all of our magnetic simulations, energy is redistributed such that the sum of the kinetic and magnetic energy is less than the total kinetic energy KE_0 contained in case H. The net energy deficit can be attributed primarily to the reduction in strength of the differential rotation by Maxwell stresses. This means that in a convection zone the way the energy is redistributed among and within the different reservoirs is modified by the presence of magnetic field, but these modifications remain moderate in the case presented here. In addition our choice of magnetic boundary conditions (potential field) could explain for some part the decrease of KE+ME since it correspond to a net Poynting flux at the boundaries.

A detailed analysis of the redistribution of ME within its mean and fluctuating components reveals that the magnetic energy contained in the mean-field components ($m = 0$) represents only 2% of total ME with the 98% re-

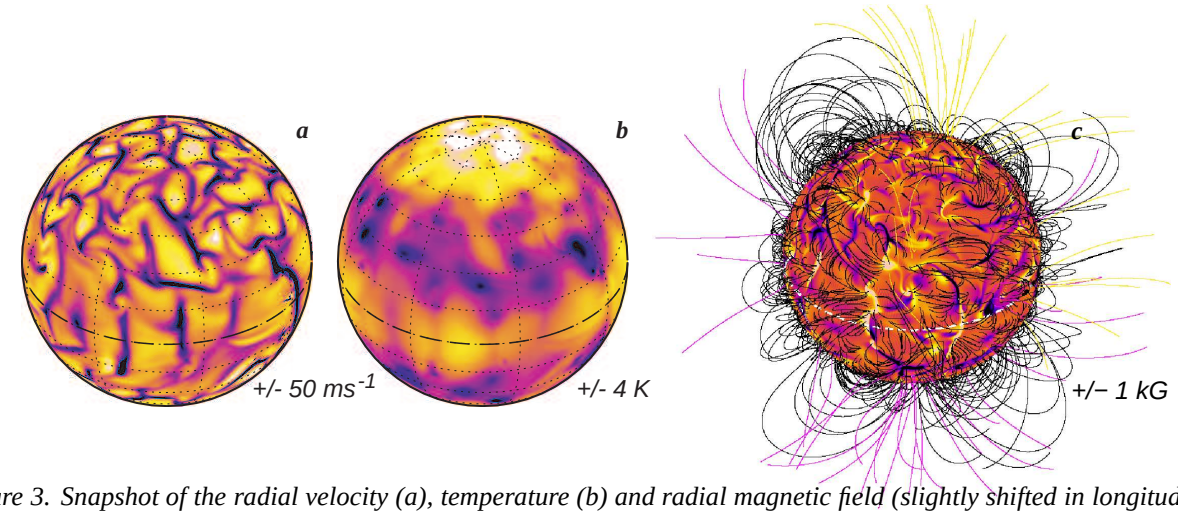

Figure 3. Snapshot of the radial velocity (a), temperature (b) and radial magnetic field (slightly shifted in longitude) (c) near the top of the domain for case M3. A potential extrapolation of the magnetic field has been superimposed on panel c), with closed magnetic loops in black, and respectively outward (inward) open fields lines in yellow (magneta). Typical field strengths are indicated, with dark tones corresponding to downward velocities and negative temperature fluctuations and polarities. The dashed line indicates the equator.

maining contained in the non-axisymmetric fluctuations. Most of the mean-field energy is in the toroidal field (1.5%), which exceeds the energy in the poloidal field by about a factor of three due to the stretching and amplification of toroidal field by differential rotation (the ω-effect). This ratio is smaller than in the Sun, where the mean toroidal field is estimated to be about two orders of magnitude more energetic than the mean poloidal field. This discrepancy can again be attributed to the absence of an overshoot region and a tachocline, where toroidal field can be stored for extended periods while it is amplified by relatively large angular velocity gradients. For the non-axisymmetric fluctuations, the magnetic energy is approximately equally distributed among the toroidal and poloidal fields, indicating that the turbulent convection can efficiently generate both components in roughly equal measure, implying that the ω-effect plays a lesser role. The radial profile of ME peaks at the bottom of the domain, due to the downward transport of magnetic fields by turbulent plumes. Magnetic fields generation through dynamo action is present at all scales, with ME being in superequipartition over degree $\ell \sim 20$.

In order to illustrate the complex interplay between convective motions, differential rotation and magnetic fields, we display the structure of the convection and magnetic fields of *M3* in Figure 3. The convective patterns are qualitatively similar to the hydrodynamic progenitor case H. The radial velocity (Fig. 2a) is dominated by narrow cool downflow lanes and broad warm upflows, with a more isotropic behavior at higher latitudes. The charactristic spatial scale here is larger than supergranulation, which is as of today, the smallest convective scale that such global models can simulate but in rather thin shell (see Derosa, Gilman & Toomre 2002). The temperature fluctuations (Fig. 2b) exhibit a banded appearance most likely linked to an inner thermal wind, that contributes somewhat to the establishment of the differential rotation (see below). The much smoother appearance of the temperature fields is due to our choice of a small Prandtl number (Pr ¡ 1). We can see that the strongest vortices correlated well with the coldest fluctuations resulting in an outward transport of heat.

The radial magnetic field (Fig. 2c) is found to be concentrated in the downflow lanes, with both polarities coexisting having beed swept there by the horizontal diverging motions at the top of the domain. The Lorentz forces in such localized regions have a noticable dynamical effect on the flow, with ME sometimes being locally bigger than KE, influencing the evolution of the strong downflow lanes via magnetic tension that inhibits vorticity generation and reduces the shear. The magnetic field and the radial velocity possess a high level intermittency both in time and space, revealed by extended wings in their probality distribution functions and are quite asymmetric (BMT04). The longitudinal velocity v_ϕ is much more gaussian-like. These results are in good agreement with simulations of compressible MHD turbulence in cartesian geometry (Brandenburg et al. 1996).

In Figure 2c we have also represented the potential extrapolation of the radial magnetic field at the top of the computational domain. We see that the field can take the form of magnetic loops connecting either local or widely separated areas as well as be open, with respectively outward (inward) field lines in yellow (magenta). The longitudinal magnetic field (not shown) B_ϕ appears near the surface more distributed and more patchy than B_r, characterized by relatively broad regions of uniform polarity, particularly near the equator.

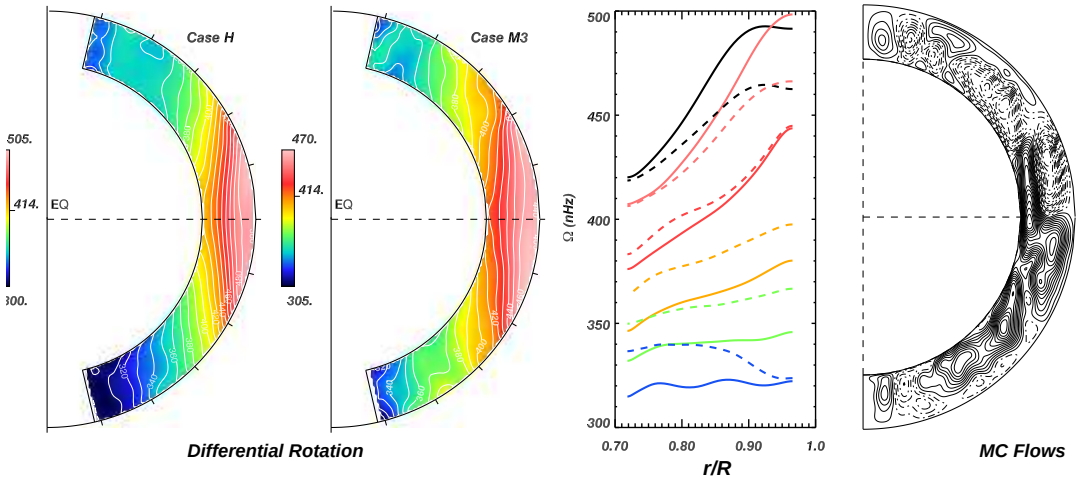

Figure 4. Left and middle panels: Temporal and longitudinal averages of the angular velocity profiles (converted to nHz) achieved in case H and $M3$ over an interval of 100 days (shown as contour plots). These cases exhibit a prograde equatorial rotation and a strong contrast $\Delta\Omega$ from equator to pole, as well as possess a high latitude region of particularly slow rotation. In the middle right panel, displaying radial cuts of Ω (with the equatorial cut on top and decreasing latitudes as we go down) for both cases, the reduction in $\Delta\Omega$ due to the nonlinear feed back of the Lorentz forces (solid vs dashed lines) can be assessed. Right panel: Temporal and longitudinal average of the meridional circulation realized in case M3 (shown in a meridional cross section view). The intricate profile with the presence of multi cells both in radius and latitude is clearly visible. Clockwise circulations are shown as solid contours. Typical velocity are about 25 ms^{-1}.

3.2. Differential Rotation and Meridional Circulation

Helioseismic inversions of large-scale, axisymmetric, time-averaged flows in the Sun currently provide the most important observational constraints on global-scale models of solar convection. Such flows (averaged over longitude and time) have therefore been a primary focus of simulations of the solar convection zone (Glatzmaier 1987; Miesch et al. 2000; Brun & Toomre 2002, Miesch, Brun & Toomre 2005). Of particular importance and reasonnably well constrained by helioseismology, is the mean longitudinal flow, i.e. the differential rotation $\Omega(r,\theta)$, which is characterized by a fast equator, slow poles and a profile almost independant of radius at mid latitudes (Thompson et al. 2003).

In Figure 4 (left panel), we display the time-averaged angular velocity profile achieved in the purely hydrodynamic case H. This case possesses a fast equator, a monotonic decrease of Ω with latitude and some constancy along radial line at mid latitudes, all these attributes being in reasonnable agreement with helioseismic inferences. With fairly strong magnetic fields sustained within the bulk of the convection zone in case *M3*, it is to be expected that the differential rotation Ω established in the progenitor case H will respond to the feedback from the Lorentz forces. Figure 4 (middle left panel) shows the time-averaged angular velocity achieved in case *M3*, which exhibits a prograde equatorial rotation with a monotonic decrease in angular velocity toward higher latitudes as in the Sun. The main effect of the Lorentz forces is to extract energy from the differential rotation. The kinetic energy contained in the differential rotation drops by a factor of two after the addition of magnetic fields and this decrease accounts for over 70% of the total kinetic energy difference found between the two cases (see above). This is reflected by a 30% decrease in the angular velocity contrast $\Delta\Omega$ between the equator and latitudes of 60°, going from 140 nHz (or 34% compared to the reference frame Ω_o) in the hydrodynamic case H to 100 nHz (or 24%) in case *M3*. This value is close to the contrast of 22% inferred from helioseismic inversion of the solar profile (Thompson et al. 2003). Thus the convection is still able to maintain an almost solar-like angular velocity contrast despite the inhibiting influence of Lorentz forces.

A careful study of the redistribution of the angular momentum in our shell reveals that the source of the reduction of the latitudinal contrast of Ω can be attributed to the poleward transport of angular momentum by the Maxwell stresses (see Brun 2004, BMT04). The large-scale magnetic torques are found to be 2 orders of magnitude smaller, confirming the small dynamical role played by the mean fields in our MHD simulation. The Reynolds stresses now need to balance the angular momentum transport by the meridional circulation, the viscous diffusion and the Maxwell stresses. This results to a less efficient speeding up of the equatorial regions. Since ME in case *M3* is only 7% of KE, the Maxwell stresses are not yet the main players in redistributing the angular mo-

mentum and case $M3$ is able to sustain a strong differential rotation as observed in the present Sun. At higher level of magnetism with ME near equipartition with KE, the differential rotation is severely damped and no more solar-like. The somewhat faster rotation rate and larger $\Delta\Omega$ in case H relative to case *M3* further suggests that a reduced level of the Sun's magnetism (as during the Maunder minimum) may lead to greater differential rotation. Some evidence seem to confirm it (Eddy et al. 1976, Brun 2004).

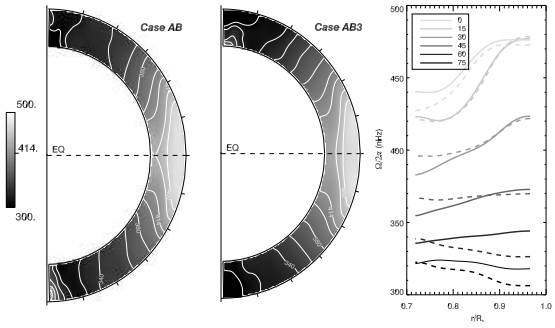

Figure 5. as in Figure 4, but for cases AB and AB3 (see text and Miesch, Brun & Toomre 2005): The tilting in case AB3 of the isocontour of Ω to become constant along radial lines at mid latitudes (due to the baroclinic forcing imposed at the bottom BC) is clear when comparing dashed vs solid cuts in the right panel.

There is actually some debates on the relative importance of the thermal wind linked to baroclinic effects compared to the Reynolds stresses in establishing the solar differential rotation. Several authors (Rudiger & Kitchatinov 1995, Robinson & Chan 2001, Durney 1999) advocate that the thermal wind (cf. Pedlosky 1987, Brun & Toomre 2002, Miesch, Brun, Toomre 2005) dominates the delicate balance that leads to the observed angular velocity profile. In our 3–D simulations we do find that the thermal wind account for a fraction of the differential rotation profile in the bulk of the convection zone, but there are many locations, mainly close to high shearing regions, where it does not. In our simulations, convection redistribute heat and angular momentum both in radius and latitude and establish latitudinal gradients of temperature and entropy compatible with a differential rotation. Rempel (2005) advocated that a thermal forcing due to the presence of a tachocline could influence the profile of Ω, by bending the isocontour lines toward radial profiles. By enforcing a thermal wind balance at the bottom BC of a 3-D purely hydrodynamical convective model (case AB3), Miesch, Brun & Toomre (2005), showed as well that the solar differential rotation could be influenced by baroclinic or thermal forcing at the base of the convection zone and the forced model could be closer to helioseismic inversion by being more radial at mid-latitude (see Figure 5). The exact nature of this thermal balance due either to the influence of the tachocline or to turbulent convective latitudinal heat transport or both effects, still need to be modelled in greater details by having even more realistic simulations of the solar turbulent convection zones. The near constancy of the isocontours of Ω along radial lines could be used in turn to assess the radial structure of the tachocline if this boundary layer is assumed to be in strict thermal wind balance.

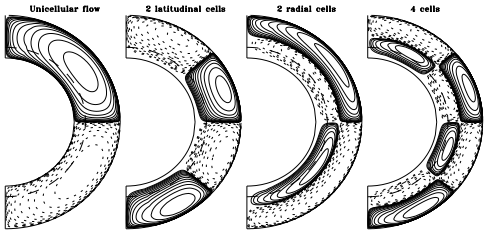

Figure 6. Different type of multicellular meridional flow patterns in 2D mean field models of the solar cycle as considered by Jouve & Brun (2005), with dotted (solid) contours denoting (anti-)clockwise circulation, and the dashed line the base of the convective zone.

In Figure 4 (right panel) we display the meridional circulation realized in case *M3*. This meridional circulation is maintained by buoyancy forces, Reynolds stresses, pressure gradients, Maxwell stresses, and Coriolis forces acting on the differential rotation. Since these relatively large forces nearly cancel one another, the circulation can be thought as a small departure from (magneto)-geostrophic balance, and the presence of a magnetic field can clearly influence its subtle maintenance. In case *M3*, but also in our purely hydrodynamical cases, the meridional circulation exhibits a multi-cell structure both in latitude and radius, and possesses some asymmetry with respect to the equator. Over the temporal period sampled, two vertical cells are present at low latitudes in the northern hemisphere whereas only one, with a rather irregular shape, is present in the southern hemisphere. Other temporal samplings reveal different profiles but in the large they all possess multi-cell structures. Since the convection possesses some asymmetry (cf. Fig. 3) it is not surprising that the meridional circulation does the same.

The shape of the meridional circulation is an important ingredient of solar dynamo models of the flux transport type. These models are usually built with one large-scale circulation (per hemisphere) and the speed of the flow is used to control the timing of the solar cycle. The presence of two meridional cells with latitude, as revealed by local helioseismology for the northern hemisphere (Haber et al. 2002) or anticipated with our 3-D models, does not seem as problematic for solar dynamo models of the flux transport type (Dikpati et al. 2004), as two meridional cells with radius could actually be. Indeed Jouve & Brun (2005) have recently considered such a situation in 2-D mean field flux transport type model (Figure 6). They found that several cells in radius significantly reduce the cycle period compared to model using only one large cells. Mixed models possessing several meridional cells both with latitude and radius exhibit more sophisticated butterfly patterns and long cycle period as well, the presence of several cells in radius setting predominatly the cycle period. Precise inversions of the meridional circulation down to the tachocline are thus needed.

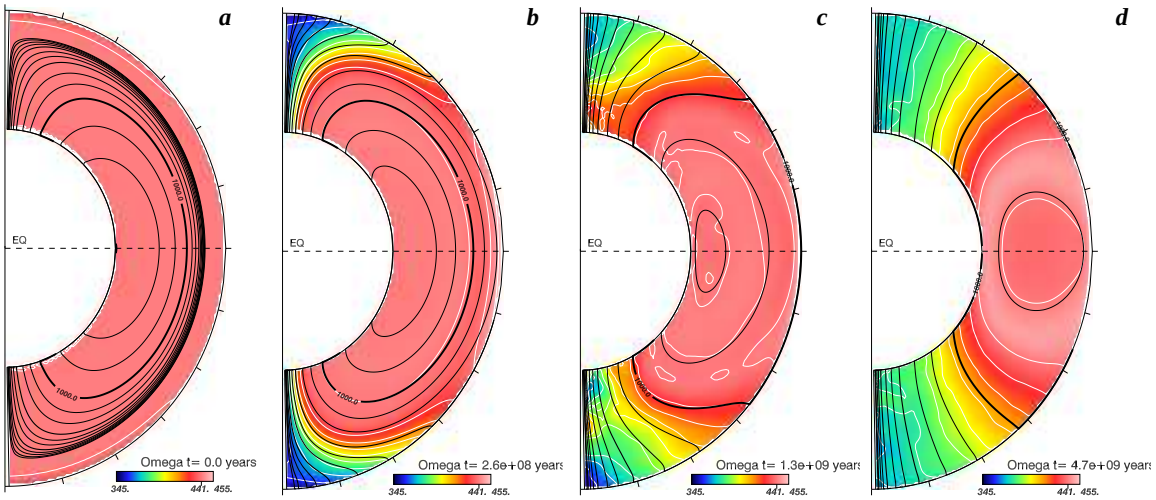

Figure 7. Temporal evolution of the angular velocity Ω (color contours) and the mean axisymmetric poloidal field (superimposed black lines) for a deeply confined fossil magnetic field. **a-d)** *sequence spanning 4.7 Gyr of the dipolar magnetic field in the presence of rotation and shear. We note the connection of the field lines with the imposed top shear and the resulting Ferraro law of isorotation at latitude greater than 40-45°.*

3.3. Solar Magnetism and Radiative Interior

We now turn to considering the magnetohydrodynamical processes acting in the solar radiative interior and in the tachocline inspired by the work of Gough & McIntyre (1998) (see also Rudiger & Kitchatinov 1997, McGregor & Charbonneau 1999, Garaud 2002), i.e a latitudinal shear is imposed on top of a stable radiative zone, and we expect a fossil dipolar magnetic field to prevent that shear for propagating inward. Other processes such as anisotropic turbulence in the overshooting layer could also be invoked (see Spiegel & Zahn 1992). We consider here the time-dependent problem, starting from various initial conditions, and this for two reasons: i) both the tachocline spread and the diffusion of the magnetic field proceed very slowly, and thus it is not clear that a stationary solution can be reached by the age of the Sun; ii) such a stationary solution may not be unique, but it may actually depend on the initial conditions.

Two important hypothesis of our work are that we let the poloidal field diffuse, and that the tachocline circulations are driven mainly by thermal (not viscous) diffusion, as in the Sun (see Brun & Zahn 2005). Moreover, we use for our simulations the 3-dimensional code ASH (see above but without the term proportional to $\boldsymbol{\nabla} S$ in the energy equation) and resolve the Alfvén crossing time; this enables us to describe non-axisymmetric hydrodynamical instabilities which may lead to drastic reconfigurations of the magnetic field, as was recently demonstrated numerically by Braithwaite and Spruit (2004), following the pioneering work of Tayler (Tayler 1973 and collaborators).

We have studied several magnetic field configurations in the solar radiative interior in order to assess if the shear of the tachocline will or will not spread inward and reach a thickness much larger than inverted by helioseismic technics (i.e $h < 0.05R$). We actually find that the field always connect to the shear, and that burying it just delay in time the reconnection. In the case presented Figure 7, the magnetic field lines are confined below $r = R_B < r_{\rm top}$, to let the tachocline penetrate into the interior before encountering the fossil field (Fig. 7a). When the field lines make contact with the shear (see Fig. 7b), we notice a fast increase of the mean toroidal energy in a thin latitudinal band, which corresponds to the magnetopause anticipated by Gough & McIntyre. However the existence of this magnetic layer does not prevent the field lines to connect to the imposed latitudinal shear, and to establish in an Alfvenic time scale a differential rotation in the radiative interior. Since this is not observed (inverted) in the Sun, this scenario of the magnetic confinement of the tachocline seems in difficulty. An interesting result found by the nonlinear calculations of Brun & Zahn (2005), is that it is unlikely that inside the radiative zone of the Sun the magntic field topology is as simple as a pure dipole. It is most likely in a mixed poloidal-toroidal configuration (as anticipated with a linear approach by Tayler 1973), with the two components of the field being roughly of the same amplitude. How this inner field interact with the dynamo field is a very interesting questions that need to be studied in details and we have started to do so.

4. PERSPECTIVES

We have shown that numerical simulations of the complex internal solar magnetoydrodynamics are becoming more and more tractable with today's supercomputers. In particular we have studied how turbulent convection under the influence of rotation can establish a strong differential rotation and weak meridional circulation, generate magnetic fields through dynamo action and how

Lorentz forces act to diminish the differential rotation by having Maxwell stresses transporting angular momentum poleward and thus opposing the Reynolds stresses. Many challenges remain, among them the understanding of the two shear layers present at the base (the tachocline) and at the top of the solar convection zone is a priority since these layers are directly linked to the solar dynamo (Ossendrijver 2003) and subsurface weather (Haber et al. 2002). Another challenge is to get a more accurate and deeper inversion of the meridional circulation present in the solar convection since it plays a crucial role in current mean field solar dynamo models (Dikpati et al. 2004, Jouve & Brun 2005). Our numerical simulations favor a multi-cells structure for the meridional circulation whereas flux transport models assume one large cell. Multi-cellular meridional flow in radius tends to slow down greatly the period of transport-flux type dynamos and it would be difficult to reconcile this models with observations, if such flow were indeed present in the Sun. This issue need to be clarified. In order to progress in our understanding of the solar interior, we have started to study with ASH in three dimensions, the solar tachocline and radiative zone (Brun & Zahn 2005). We have considered how a dipolar magnetic field could oppose the radiative spread of the tachocline. We have found that independantly of the degree of confinement of the fossil magnetic field it will diffuse into the convection zone and communicate to the radiative interior, first, at high, then at lower latitudes, the differential rotation, therefore enforcing an isorotation of Ω along the poloidal field lines. This behavior is known as Ferraro's law of isorotation. Work is in progress to compute with ASH in one single global model the solar convection and radiation zones. These simulations will provide a first step toward a self-consistent, high resolution model of the solar dynamo.

We are thankful to the organisers for inviting us. The results presented in this paper have been obtained in collaboration with many colleagues, in particular, M. Miesch, J. Toomre, J.P. Zahn and with my PhD student L. Jouve.

REFERENCES

[1] Brainwaith, J. & Spruit, H. C. 2004, Nature, 431, 81

[2] Brandenburg, A. 2005, ApJ, 625, 539

[3] Brandenburg, A., Jennings, R. L., Nordlund, Å., Rieutord, M., Stein, R. F., Tuominen, I. 1996, JFM, 306, 325

[4] Brun, A. S. 2004, Solar Phys., 220, 333

[5] Brun, A. S., & Toomre, J. 2002, ApJ, 570, 865

[6] Brun A. S., & Zahn, J.-P. 2005, A&A accepted

[7] Brun, A. S., Antia, H. M., Chitre, S. M. & Zahn, J.-P. 2002, A&A, 391, 725

[8] Brun, A. S., Miesch, M. S. & Toomre, J. 2004, ApJ, 614, 1073 (BMT04)

[9] Cattaneo, F. & Hughes, D. W. 2001, Astron. & Geophys., 42, 3, 18

[10] Charbonneau, P., 2005, Living Rev. Solar Phys., 2

[11] Clune, T. L., Elliott, J. R., Glatzmaier, G. A., Miesch, M. S., & Toomre, J. 1999, Parallel Comput., 25, 361

[12] DeRosa, M. L., Gilman, P. A. & Toomre, J. 2002, ApJ, 581, 1356

[13] Dikpati, M. & Charbonneau, P. 1999, ApJ, 518, 508

[14] Dikpati et al., 2004, ApJ, 601, 1136-1151

[15] Durney, B. R. 1999, ApJ, 511, 945

[16] Eddy, J. A., Gilman, P. A. & Trotter, D. E. 1976, Solar Phys., 46, 3

[17] Garaud, P. 2002, MNRAS, 329, 1

[18] Gilman, P. A. 1983, ApJS, 53, 243

[19] Glatzmaier, G. A. 1987, in The Internal Solar Angular Velocity, ed. B. R. Durney & S. Sofia (Dordrecht: D. Reidel), 263

[20] Gough, D. O. & McIntyre, M. E. 1998, Nature, 394, 755

[21] Haber, D. A., Hindman, B. W., Toomre, J., Bogart, R. S., Larsen, R. M., & Hill, F. 2002, ApJ, 570, 855

[22] Jouve, L. & Brun, A.S. 2005, SF2A05, in press

[23] Judge 2003, in The Future of Cool-Star Astrophysics, eds. A. Brown, G. M. Harper, & T. R. Ayres, Cool Stars Meeting XII, 158

[24] Kichatinov, L. L., & Rüdiger, G. 1995, A&A, 299, 446

[25] MacGregor, K. B. & Charbonneau , P. 1999, ApJ, 519, 911

[26] Miesch, M. S. , Brun, A. S., & Toomre, J. 2005, ApJ accepted

[27] Miesch, M. S., Elliott, J. R., Toomre, J., Clune, T. L., Glatzmaier, G. A., & Gilman, P. A., 2000, ApJ, 532, 593

[28] Moffatt, H. K. 1978, Magnetic Field Generation in Electrically Conducting Fluids, (Cambridge: Cambridge Univ. Press)

[29] Ossendrijver, M. 2003, Astron. Astrophys. Rev., 11, 287

[30] Pedlosky, J., 1987, Geophysical Fluid Dynamics (New York: Springer)

[31] Parker, E. N. 1993, ApJ, 408, 707

[32] Rempel, M. 2005, ApJ, 622, 1320

[33] Robinson, F. J. & Chan, K. L. 2001, MNRAS, 321, 723

[34] Rudiger & Kitchatinov 1997, Astron. Nach., 318, 273

[35] Spiegel, E. A. & Zahn, J.-P. 1992, A&A, 265, 106

[36] Stix, M. 1976, A&A, 47, 243

[37] Tayler, R. J. 1973, MNRAS, 161, 365

[38] Thompson, M. J., Christensen-Dalsgaard, J., Miesch, M. S. & Toomre, J. 2003, Ann. Rev. Astron. Astrophys., 41, 599

[39] Tobias, S. M., Brummell, N. H., Clune, T.L. & Toomre, J. 2001, ApJ, 549, 1183

[40] Weiss, N. O. 1994, in Lectures on Solar and Planetary Dynamos, ed. M. R. E. Proctor & A. D. Gilbert (Cambridge: Cambridge Univ. Press), 59